Effects of Typical Soil and Stratification Thickness on Water Infiltration Characteristics in Central Ningxia

Tianwen ZHANG[1]*, Wei CHEN[1], Xiaoying CHEN[2,3], Rongjun ZHI[1], Lin CHEN[2,3], Haibo ZHANG[1], Wei LIANG[1]

1. Ningxia Hui Autonomous Region Institute of Mineral Geology, Yinchuan 750021, China; 2. Key Laboratory of Restoration and Reconstruction of Degraded Ecosystems in Northwest China, Ministry of Education (Ningxia University), Yinchuan 750021, China; 3. College of Ecology and Environment, Ningxia University, Yinchuan 750021, China

Abstract In order to compare the influence of different soil types and stratification on water infiltration capacity, two main types of soil in the desert steppe, sierozem (S) and aeolian sandy soil (A), were selected, and infiltration simulation tests were conducted on homogeneous soil and layered soil (layer thickness 5, 10, and 20 cm), respectively. The results show that during the whole experiment, there was a small difference between S5A95 (aeolian sandy soil 95 cm thick was covered with sierozem 5 cm thick) and S10A90 (aeolian sandy soil 90 cm thick was covered with sierozem 10 cm thick) in the wetting front process, infiltration rate and cumulative infiltration, but there was a significant difference between S5A95 and S20A80 (aeolian sandy soil 80 cm thick was covered with sierozem 20 cm thick). In the initial infiltration stage, there was no significant difference between A5S95 (sierozem 95 cm thick was covered with aeolian sandy soil 5 cm thick) and A10S90 (sierozem 90 cm thick was covered with aeolian sandy soil 10 cm thick). However, with the increase of infiltration time, the wetting front process, A5S95, A10S90 and A20S80 had significant differences in terms of wetting front process, infiltration rate and cumulative infiltration. The infiltration capacity of A was significantly higher than that of S. Combined with linear R^2 value and model parameters, the three infiltration models were comprehensively compared, and the fitting process and results of the general empirical model for the infiltration process of homogeneous soil and layered soil showed good results. Three models were used to simulate the water infiltration process of layered soil with different textures, and the order of the effect is as follows: general empirical model > Kostiakov model > Philip model. Soil type and layer thickness had a great influence on water infiltration process. When sierozem was covered with aeolian sandy soil 20 cm thick, the infiltration capacity was the best. As aeolian sandy soil was covered with sierozem 10 cm thick, the infiltration effect was the worst. Therefore, once coarse graying occurs on the surface of sierozem (the thickness of sand is more than 20 cm) or when the content of fine particles overlying aeolian sandy soil (the thickness of silt and clay soil is more than 10 cm) during ecological restoration is high, the soil hydrological characteristics will change significantly, which may lead to changes in vegetation types and even ecosystem structure.

Key words Soil type; Layer thickness; Water infiltration; Desert steppe

DOI 10.19547/j.issn2152 - 3940.2024.04.016

As an important driving factor in arid and semi-arid areas, soil water plays a significant role in soil - plant - atmosphere continuum (SPAC), directly affecting gas exchange, energy cycle and material flow in a region[1]. The desert steppe in Ningxia is located in an arid and semi-arid climate zone, and the availability of water limits the function of grassland habitat system[2]. Infiltration is the key process for rainfall or irrigation water to enter soil, and it is the central link of the "five kinds of water" transformation[3], influencing the migration, storage and circulation of water in soil[4]. As a key link in the ecohydrological cycle between the interface of soil, vegetation canopy and atmosphere (SVAT)[5], the physical and chemical characteristics and permeability coefficient of soil determine the effective infiltration efficiency of soil to precipitation, and also affect the morphology of rainfall slopes and gully flow and the erosion degree of surface soil[6].

Received: June 13, 2024 Accepted: July 23, 2024

Supported by the Natural Science Foundation of Ningxia Hui Autonomous Region (2022AAC03661); Financial Project of Geological Bureau of Ningxia Hui Autonomous Region (NXCZ20220201).

* Corresponding author.

In nature, soil is mostly characterized by cross-distributed layered structures, so soil profile structure[7] also presents different characteristics with the change of weathering, transport, deposition and other processes, and soil profile structure is an important parameter affecting soil water transport. In 1962, Chen Shuai *et al.*[8] used the coupled hydrology - crop growth relationship model to analyze the infiltration process of water in layered soil, and found that soil heterogeneity and sudden changes in the vertical interface of infiltration were important factors affecting its infiltration. In 1972, Hill *et al.*[9] put forward the phenomenon of "a finger-shaped runner", which refers to the process of water briefly lingering at the fine-coarse interface and then rapid infiltration when fine soil is located on top of coarse soil in the soil profile.

In layered soil, geological forces and biological activities will change soil structure and composition, resulting in a large gap between the water infiltration process of layered soil (heterogeneous) and homogeneous soil[10]. The water flow theory of Darcy's law in hydrology can no longer describe the water infiltration and redistribution of layered soil well. Domestic and foreign scholars have also carried out a large number of experiments and theoretical studies on the water transport process and infiltration rule in lay-

ered soil[11]. Romano *et al.*[12] proposed that the structure composed of upper coarse soil and lower fine soil can effectively increase the infiltration capacity of soil water, retain water and prevent evaporation. Hillel *et al.*[13] and Zhao Peilun[14] pointed out that for the layered soil composed of upper fine grained soil and lower coarse grained soil, the water capacity of fine grained soil increased due to the effect of capillary water in the soil.

Ren Lidong *et al.*[15] proposed that the infiltration performance of layered soil was the best when the layer thickness reached 5 cm. A large number of field experiments have proved that the main water of herbaceous plants is from soil at a depth of 10 – 20 cm, and in years with less rainfall, herbaceous plants have a significant impact on soil water at a depth of 0 – 20 cm[16-17]. At present, most studies on the water infiltration of uneven layered soil focus on the changing characteristics under different layering order and layering quantity, and there are few studies on the influence of the type and layering thickness of layered soil on the infiltration process of soil water. Among them, Huang *et al.*[18-20] selected interlayered coarse layered soil (different layer combinations and quantity) to conduct field soil water infiltration experiments, which has certain reference significance. However, soil hydrological process is a comprehensive coupled process involving multiple factors, and the influence of different types and layers of layered soil on water infiltration needs to be explored more.

The zonal calcareous soil formed in the desert steppe of Ningxia accounts for 25.2% of the soil area of Ningxia[21]. Rainfall, topography and human activities have led to large-scale desertification of desert steppe in Ningxia, forming a large number of sand-covered lime soil and even aeolian sand soil. In the past 40 years, especially in the past 20 years of ecological governance, the soil has gradually recovered in the remarkable recovery of vegetation, and the fine-grained soil layer on the surface of soil has gradually formed and thickened. The change of hydrological characteristics caused by the change of soil surface structure is extremely important for scientific desertification control and vegetation restoration. Therefore, the water infiltration of typical sierozem and aeolian sandy soil in the desert steppe belt of central Ningxia was studied through an indoor soil column test, and the water infiltration process and changing rule of layered soil with different layer thickness were analyzed. Three models were used to analyze the difference of water infiltration process and reveal the infiltration capacity of layered soil. It provides theoretical basis for the environmental protection and ecological restoration of desert steppes.

1 Materials and methods

1.1 Experimental samples Typical soil samples were selected from Yanchi County, Ningxia Hui Autonomous Region, and the region belongs to the desert steppe belt in the middle of Ningxia. The collected soil was sierozem and aeolian sandy soil, and the sampling depth was 0 – 40 cm. After the collected soil samples were naturally air-dried, vegetation roots and large impurities were removed from the soil , and the soil was ground by a 2 mm sieve for reserve use. The basic information of the sampling area is shown in Table 1.

Table 1 Basic situation of the sampling area

Soil type	Percentage of soil particles of different sizes//%		
	Clay	Silt	Sand
Sierozem	40.27 ±0.30	29.19 ±0.49	31.52 ±0.72
Aeolian sandy soil	8.29 ±0.04	19.73 ±0.74	71.97 ±0.79

1.2 Experimental apparatus The main instruments used in the soil column infiltration test included soil columns, Markov bottles, glass tubes and stands. The Markov bottles were 10 cm in outer diameter, 9 cm in inner diameter, 50 cm in height, and 3 179.25 cm^3 in volume. The soil columns were 3.8 cm in radius, and 100 cm in height. The outer diameter of the glass tubes was 0.8 cm, and their inner diameter was 0.6 cm. The material of the soil columns and Markov bottles: transparent PE pipes 10 mm thick. A water inlet was at the top, and a water outlet was at the bottom.

1.3 Experimental design The experiment was carried out in the Key Laboratory of Restoration and Reconstruction of Degraded Ecosystems in Northwest China, Ministry of Education (Ningxia University). Different soils were combined and filled into the soil column tubes (Fig. 1). A total of 8 treatments were set up, and each treatment had 3 replicates, so there were a total of 24 soil columns. Among them, there were 6 kinds of layered soil columns, and the stratified thickness was 5, 10 and 20 cm, respectively.

1.4 Test process

1.4.1 Process of infiltration test. Before the test, the air tightness of Martensier bottles should be checked. In case of gas leakage, petroleum jelly can be applied to seal them, and a scale line of 0 – 50 cm can be set on the outside of the Markov bottles to visually record the change of water level[21].

Before loading the soil, to eliminate the dominant flow on the wall of the soil columns, petroleum jelly was smeared evenly on the inner wall. A scale line of 0 – 100 cm was pasted on the wall of soil columns to observe the infiltration process of wetting front. The bulk density of the soil was 1.4 g/cm^3, and the bottom end of soil columns was built with asbestosed wire gauze and gauze to prevent the leakage of soil particles. In the soil column pipes, the distance was 20 cm, and the soil tamper was used for compaction. In order to effectively avoid structural water pressure sudden change at the interface, the soil layer was bristled with a brush after each compaction and filled to 1 m. Finally, a filter paper was used to cover the surface of the soil to facilitate the uniform infiltration of soil water.

In the experiment, in order to reduce the atmospheric evaporation of topsoil water, the interior of the laboratory was shaded, and windows and other vents were closed. When infiltration began, a stopwatch was used to record time. The water level of Markov bottles and position of wetting front were recorded continuously after 0 – 5 min (1 time/30 s), 5 – 15 min (1 time /1 min), 15 – 30 min (1 time/3 min), 30 – 60 min (1 time/5 min), 60 –

120 min (1 time/10 min), and after 120 min (1 time/30 min). Each experiment was repeated three times.

The final wetting front distance was the average distance of 3 wetting front points read from 3 directions of soil columns respectively. The average of soil infiltration rate 5 min before infiltration was as the initial infiltration rate[24].

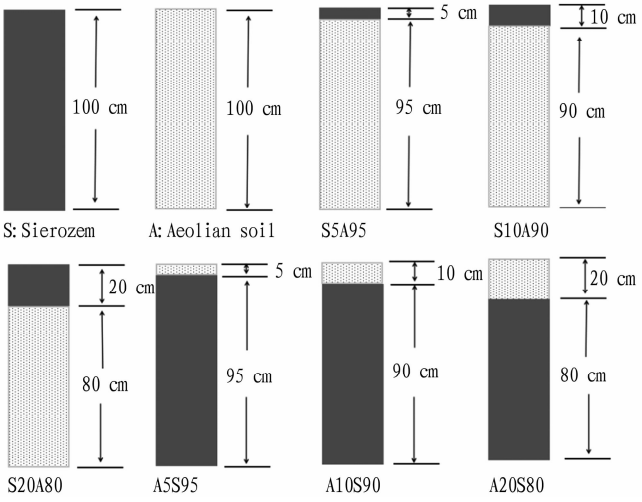

Fig. 1 Soil stratification structure map

1.4.2 Infiltration models.

(1) Kostiakov formula:

$f(t) = at^b$

In the formula, $f(t)$ is infiltration rate (mm/min); t is time (min); a and b are model parameters obtained by the experiment[24].

(2) Philip formula:

$f(t) = 0.5St^{-0.5} + f_c$

In the formula, $f(t)$ is infiltration rate (mm/min); S is a model parameter obtained by the experiment; t is time (min); A is the steady infiltration rate of soil (mm/min).

(3) General empirical formula[24]:

$f(t) = a_1 + b_1 f^{-n}$

In the formula, $f(t)$ is infiltration rate (mm/min); t is time (min); a_1, b_1 and n are model parameters obtained by the experiment.

(4) Linear fitting model[24]:

$I = ax_f$

$i = b/x_f$

In the formula, I is the cumulative infiltration amount (mm); i is the infiltration rate (mm/min); x_f is the distance of wetting front; a and b are model parameters obtained by the experiment[21].

1.5 Data analysis After the experimental data was sorted out, Excel was used for graph drawing, and linear fitting was performed with Origin9.3. One-way ANOVA was performed on the data, and SPSS 18.0 was used for the statistical analysis of the data, with the significance level of 0.05.

2 Results and analysis

2.1 Variation characteristics of wetting front It can be seen from Fig. 2 that 8 different soils and stratified soil columns had different characteristics of wetting front processes. Within 0 – 20 min after the beginning of infiltration, the wetting front curves of S5A95 and S10A90 overlapped, that is, there was a small difference in the wetting front curves as 5 – 10 cm sierozem covered aeolian sandy soil. The wetting front process of S20A80 was lower than the previous two, proving that the wetting front process was inversely proportional to the thickness of sierozem. When sierozem was overlaid with aeolian sandy soil, the overall wetting front process was higher than that of the first 4 soil columns. Among them, the wetting front process of A10S90 was 32% higher than that of A5S95, and that of A20S80 was 68% higher than that of A5S95. After the infiltration was conducted for 60 min, there was a very significant difference between A, S5A95, S10A90 and S20A80 ($P < 0.01$), and the height of wetting front was 64.72, 34.26, 26.81 and 19.57 cm, respectively. That of S, A5S95, A10S90 and A20S80 was 19.45, 24.75, 26.07, and 35.30 cm, respectively, and there were very significant differences among all treatments ($P < 0.01$), but there was no significant differences between A5S95 and A10S90. At 120 min, the position of wetting front process in each treatment was as follows: A (77.40 cm) > S5A95 (61.03 cm) > S10A90 (46.81 cm) > S20A80 (33.24 cm), A20S80 (41.07 cm) > A10S90 (31.78 cm) > A5S95 (30.87 cm) > S (27.63 cm). It can be seen from the above results that the migration speed of wetting front rose significantly with the increase in the thickness of aeolian sandy soil on sierozem. In the initial stage of infiltration, there was no difference between the treatments with sierozem covered with aeolian sandy soil 5 and 10 cm thick ($P > 0.05$), but there was a significant difference between the former and homogeneous sierozem ($P < 0.01$). In the stable stage of infiltration, there was no significant difference in the migration process of wetting front between sierozem covered with aeolian sandy soil (5 and 10 cm thick) and homogeneous sierozem ($P > 0.05$), but there was significant difference in the migration process of wetting front between sierozem covered with aeolian sandy soil 20 cm thick and homogeneous sierozem ($P < 0.05$). However, with the increase of the thickness of sierozem on aeolian sandy soil, the migration speed of wetting front declined significantly. In the initial stage of infiltration, there was no significant difference between between sierozem covered with aeolian sandy soil 5 and 10 cm thick. Subsequently, there were extremely significant differences in the migration process of wetting front between aeolian sandy soil covered with sierozem (5, 10 and 20 cm thick) and homogeneous aeolian sandy soil ($P < 0.01$).

The variation law of wetting front process with time showed the same trend: the slope of wetting front gradually decreased with time, and the curve of wetting front was steep in the initial stage of infiltration. With the increase of infiltration time, when the wetting front crossed the interface, the migration velocity (slope) of wetting front reduced rapidly, changing from non-uniform advance to uniform advance, and the curve of wetting front gradually flattened. As can be seen from Fig. 2, the wetting front curves of S, A5S95, A10S90 and A20S80 were relatively gentle, while those of A, S5A95, S10A90 and S20A80 were steep. Soil configuration, namely soil structural form, is the arrangement of soil layers, and

affects the transport of soil water flow and solute[23]. The wetting front migration process of aeolian sandy soil was 3 times that of sierozem, mainly because sierozem is dry and has large matrix potential[24]. However, the porosity of aeolian sandy soil is large, and its matrix potential and adhesion are lower than those of sierozem. Therefore, in the initial stage of infiltration, the migration of wetting front process of sierozem and aeolian sandy soil was different under the same stratified treatment.

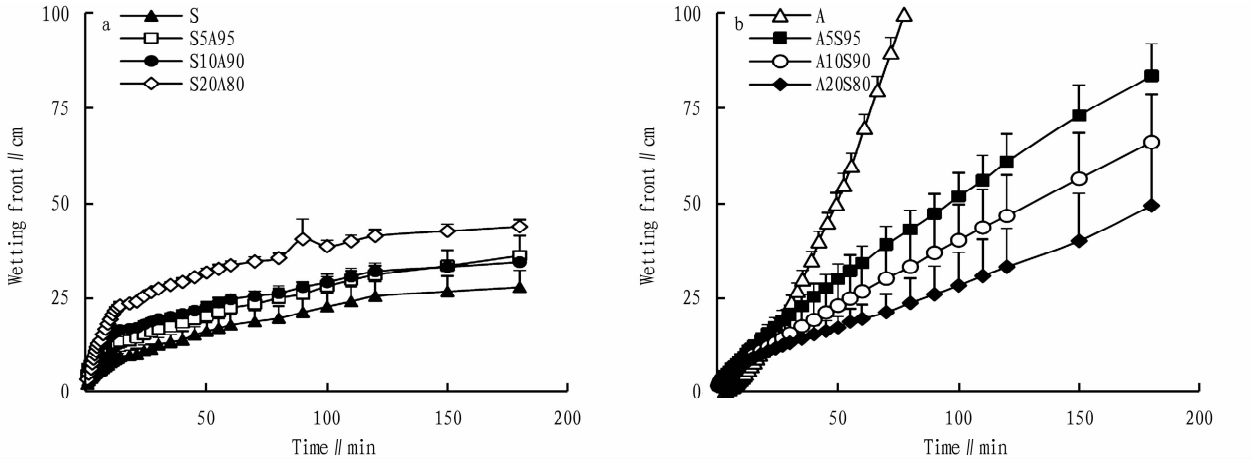

Fig. 2 Variation trend of soil wetting front

Table 2 Power function fitting parameters and soil infiltration characteristics

Treatment	Initial infiltration rate // mm/min	1-h cumulative infiltration // mm	Stable infiltration rate // mm/min	Average infiltration // mm/min	Fitting formula	R^2
S	27.56 ± 2.93 a	334.25 ± 57.69 a	2.90 ± 0.51 a	15.23 ± 1.72 a	$Y = 2.68x^{0.48}$	0.99
A5S95	30.43 ± 8.89 a	363.93 ± 48.15 a	3.56 ± 0.14 a	16.99 ± 4.51 a	$Y = 5.15x^{0.36}$	0.98
A10S90	37.31 ± 4.55 a	393.60 ± 38.68 a	3.21 ± 0.55 a	20.26 ± 2.35 a	$Y = 6.24x^{0.36}$	0.98
A20S80	41.28 ± 4.90 ab	518.65 ± 38.85 ab	4.69 ± 0.45 ab	22.99 ± 2.67 ab	$Y = 6.14x^{0.44}$	0.96
A	41.74 ± 5.18 b	864.13 ± 203.17b	14.53 ± 4.12 b	28.14 ± 4.65 b	$Y = 4.50x^{0.60}$	0.99
S5A95	27.00 ± 3.62 a	389.36 ± 31.37 a	5.25 ± 0.53 a	16.13 ± 2.23 a	$Y = 2.02x^{0.68}$	0.99
S10A90	29.32 ± 7.29 a	380.88 ± 71.66 a	4.79 ± 0.88 a	17.05 ± 4.09 a	$Y = 2.14x^{0.61}$	0.98
S20A80	26.59 ± 2.31 a	327.89 ± 59.08 a	3.95 ± 1.00 a	15.27 ± 1.66 a	$Y = 2.26x^{0.54}$	0.99

Note: Different lowercase letters after the data in the same column indicate significant differences between treatments at the 5% level.

In order to analyze the variation characteristics of wetting front over time, the power function is used to fit it:

$$H = at^b$$

where H is the distance of wetting front (cm); t is time (min); a is the infiltration depth of wetting front per unit time; b is the attenuation degree of wetting front process[21,24]. After the fitting, the order of a value in different treatments is as follows: A20S80 > A10S90 > > A5S95 > A > S20A80 > S10A90 > S5A95 > S; the order of b value in different treatments is as follows: S5A95 > S10A90 > A > S20A80 > S > A20S80 > A5S95 = A10S90. The experimental results show that a value, b value and infiltration rate were positively correlated with the thickness of aeolian sandy soil on sierozem, that is, they rose with the increase of the thickness of aeolian sandy soil. With the increase of the thickness of sierozem on aeolian sandy soil, a value increased, while b value declined. When the thickness of sierozem on aeolian sandy soil was 5, 10 and 20 cm, the infiltration rate was higher than that of homogeneous sierozem. The correlation coefficient R^2 of the eight treatments was 0.96 – 0.99, showing high reliability.

2.2 Variation characteristics of cumulative infiltration In the experiment, cumulative infiltration was used to measure the soil infiltration capacity before infiltration saturation was stable[26], and the stable infiltration rate was used to express the soil infiltration capacity after infiltration saturation was stable. It can be seen from Fig. 3 that cumulative infiltration increased greatly in the initial stage of infiltration. With the passage of time, after the infiltration stabilized, the infiltration rate began to decrease, and the slope of the cumulative infiltration curve increased first and then decreased. The difference between treatments S and A was very significant ($P < 0.001$)[21]. The order of cumulative infiltration in different treatments is as follows: A20S80 > A10S90 > A5S95 > S, and the differences were very significant ($P < 0.001$). When the infiltration was conducted for 30 min, the order of cumulative infiltration in different treatments is as follows: A (573.76 mm) > S10A90 (253.71 mm) > S5A95 (249.47 mm) > S20A80 (238.87 mm). When the infiltration time was 60 min, the order is as follows: A (864.12 mm) > S5A95 (389.36 mm) > S10A90 (380.88 mm) > S20A80 (327.89 mm), A10S90 (380.88 mm) < A5S95 (387.24 mm) < A20S80 (510.17 mm)[21]. During the whole infiltration process, the cumulative infiltration of sierozem rose with the increase in the thickness of the overlying aeolian sandy soil. When the thickness reached 20 cm, the cumulative infiltration was significantly higher than that of homogeneous sierozem ($P < 0.05$), and the cumulative infiltration of layered sierozem was higher than that of homoge-

neous sierozem. The cumulative infiltration of layered aeolian sandy soil was lower than that of homogeneous aeolian sandy soil. In the initial stage of infiltration, the cumulative infiltration of aeolian sandy soil covered with sierozem 5 cm thick was the largest. After 60 min, the cumulative infiltration of aeolian sandy soil gradually decreased with the increase in the thickness of the overlying sierozem, but there was a very significant difference between different treatments ($P<0.01$). The difference of soil physical and chemical properties and particle size characteristics was the main reason for the great difference of cumulative infiltration between sierozem soil and aeolian sandy soil under the same thickness. The results of this study were consistent with those of Gao Haiying *et al.*[27] and Xiao Qian *et al.*[28].

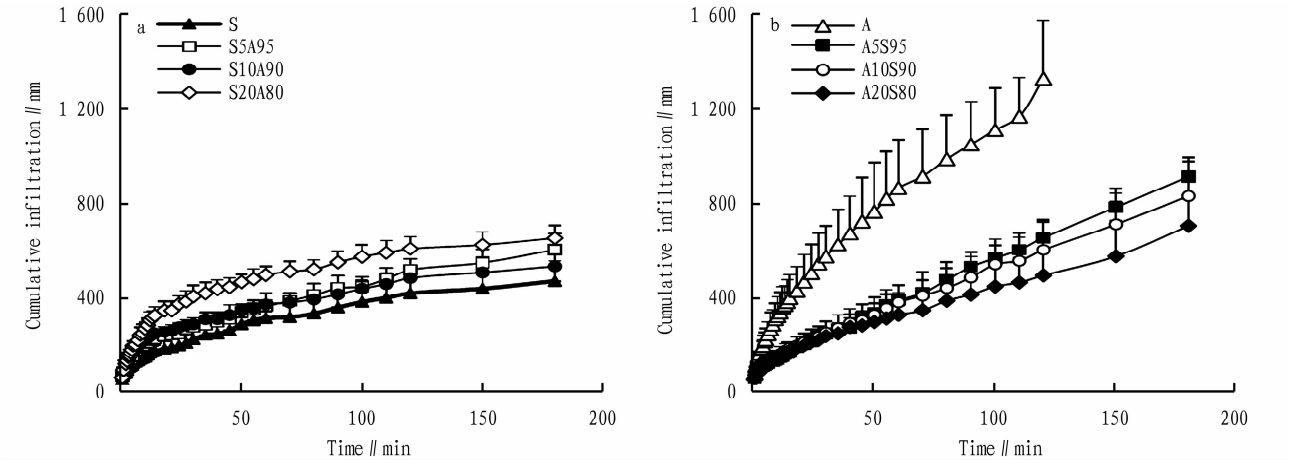

Fig. 3 Changing trend of cumulative infiltration

2.3 Fitting analysis of soil water infiltration process General empirical, Kostiakov and Philip models[29] were adopted to fit the soil water infiltration process (Table 3) to understand the soil water infiltration process of different types, so as to determine the applicability of the infiltration models.

In the Kostiakov model, a represents the initial permeability of soil, ranging from 25.25 to 92.21 here. That of homogeneous sierozem was smaller than homogeneous aeolian sandy soil (80.62 < 70.80), and the difference was significant ($P<0.05$). In the layered soil, a value rose with the increase of the thickness of aeolian sandy soil on sierozem, namely A20S80 > A10S90 > A5S95. This rule did not appear when aeolian sandy soil was covered with sierozem of different thickness. The larger the a value was, the larger the slope of the infiltration curve was, and the faster the instantaneous infiltration rate decayed. The order of instantaneous infiltration rate is as follows: A20S80 > A10S90 > A > S5A95 > A5S95 > S > S20A80 > S10A90. In the Kostiakov model, b represented the attenuation degree of infiltration rate, ranging from −0.72 to −0.37, and there was no obvious rule. R^2 was all above 0.947, indicating that the simulation results of soil water infiltration characteristics in central and eastern Ningxia using Kostiakov model were highly reliable.

In the Philip model, A is the steady infiltration rate of soil, and S stands for soil infiltration capacity. The larger the S value was, the stronger the soil infiltration capacity was. The soil infiltration capacity of different treatments is as follows: A > S5A95 > S20A80 > S > A20S80 > A10S90 > A5S95 > S10A90, and the correlation coefficient R^2 was above 0.925. The results show that the infiltration capacity rose with the increase of the thickness of aeolian sandy soil on sierozem. There was no change when the aeolian sandy soil was covered with sierozem. As the thickness of sierozem on aeolian sandy soil was 10 cm, the infiltration capacity of soil water could be significantly reduced.

In the general empirical model, a_1 represents initial infiltration rate, and b_1 represents stable infiltration rate. In the initial stage of infiltration, the simulated value differed greatly from the measured value, but the general empirical model could fit the stable infiltration stage well. When the thickness of aeolian sandy soil on sierozem reached 20 cm, the infiltration rate increased significantly. The infiltration rate significantly reduced as the thickness of sierozem on aeolian sandy soil was 10 cm, which is consistent with the results of previous studies. In the general empirical model, the determination coefficient R^2 was above 0.948, and the fitting effect was the best. The order of the fitting effect of the three models on soil water in the eastern arid region of Ningxia was as follows: general empirical model > Kostiakov model > Philip model.

2.4 Analysis of the linear regression of soil combinations and infiltration models By the linear regression fitting of the wetting front process and cumulative infiltration obtained by the soil column experiment, it can be seen that there was a good linear relationship between cumulative infiltration and wetting front process, infiltration rate and wetting front reciprocal, and wetting front square and infiltration time (Fig. 4). As shown in Table 4, a value was positively correlated with the thickness of aeolian sandy soil on sierozem. The fitting coefficient ranged from 0.942 to 0.998, so the fitting effect was good. When sierozem was covered with aeolian sandy soil (A5S95, A10S90, and A20S80), the simulation coefficient Ra^2 of cumulative infiltration and wetting front process was above 0.993. The order of b value of different treatments is A > A20S80 > A10S90 > A5S95 > S5A95 > S20A80 > S > S10A90. Coefficient b indicated infiltration rate. It can be seen from the table that infiltration rate was positively correlated with the thickness of aeolian sandy soil on

sierozem, and the maximum infiltration rate was still lower than that of homogeneous aeolian sandy soil as the thickness was 20 cm. However, the infiltration rate of soil water decreased significantly when the thickness of sierozem on aeolian sandy soil was 10 cm ($P<0.01$), indicating that the sierozem with a thickness of 10 cm could effectively maintain the low infiltration rate of soil water.

Table 3 Analysis of soil water infiltration models

Treatment	Kostiakov model			Philip model			Empirical model			
	a // mm/min	b // mm/min	R^2	S // mm/min	A // mm/min	R^2	a_1 // mm/min	b_1 // mm/min	n	R^2
S	70.80	−0.62	0.995	151.22	−5.56	0.98	−0.48	71.35	0.61	0.995
A5S95	74.59	−0.58	0.996	74.59	−0.58	0.996	−0.65	75.68	0.57	0.996
A10S90	83.39	−0.72	0.995	83.39	−0.72	0.995	2.75	79.69	0.78	0.998
A20S80	92.21	−0.51	0.993	92.21	−0.51	0.993	−6.92	99.26	0.44	0.998
A	80.62	−0.48	0.983	166.19	3.96	0.993	−1.75	88.59	0.44	0.995
S5A95	75.18	−0.68	0.993	160.71	−7.22	0.958	2.54	71.91	0.74	0.996
S10A90	25.25	−0.37	0.947	45.63	2.91	0.925	−1.88	27.04	0.32	0.948
S20A80	70.61	−0.65	0.997	151.62	−6.33	0.980	0.55	69.94	0.66	0.997

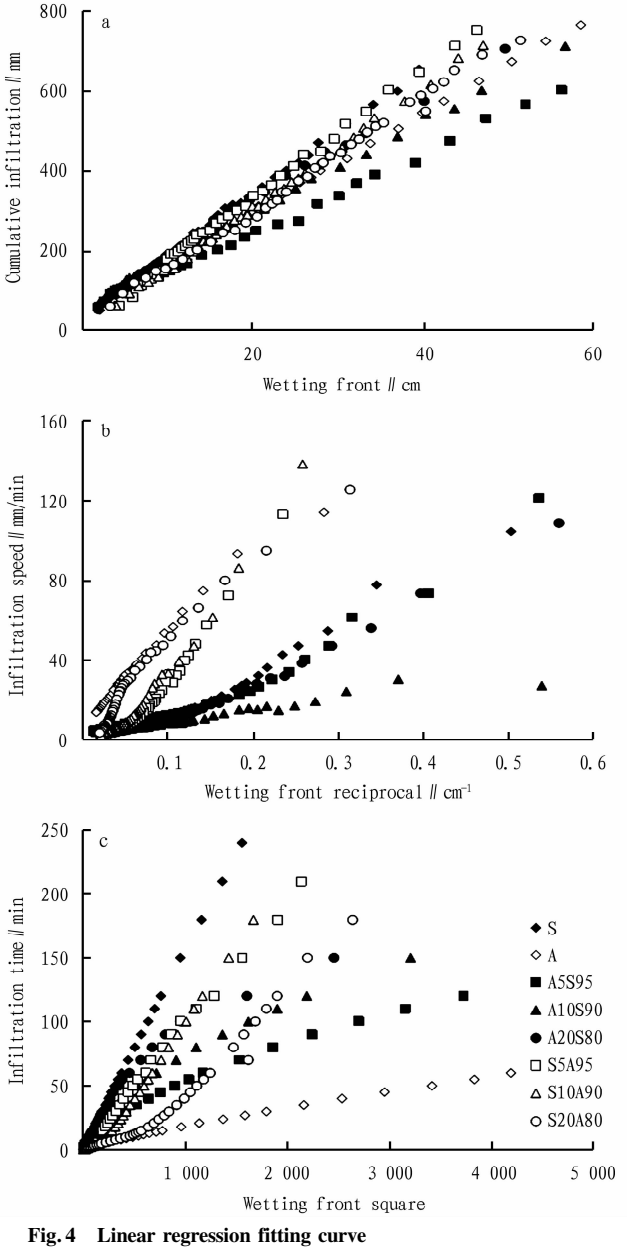

Fig. 4 Linear regression fitting curve

Table 4 Linear regression coefficient

Treatment	Coefficient a	Determination coefficient Ra^2	Coefficient b	Determination coefficient Rb^2
S	17.212	0.980	108.964	0.988
A5S95	16.593	0.996	329.236	0.821
A10S90	15.268	0.998	376.232	0.834
A20S80	14.667	0.993	456.651	0.956
A	13.699	0.987	508.566	0.881
S5A95	11.150	0.967	175.160	0.919
S10A90	13.550	0.942	72.354	0.825
S20A80	15.828	0.951	158.340	0.931

3 Discussion

In the early stage of soil infiltration, the convergence of soil water infiltration curves is large, because the soil is dry and the water potential gradient is large, and the molecular force plays a leading role. In the initial stage of infiltration, matrix potential is the main factor affecting the cumulative infiltration and advance rate of wetting front[30], and soil infiltration mainly depends on the surface adsorption of soil particles in the middle and later stages[31]. Therefore, in the first few minutes of infiltration, the infiltration rate and the cumulative infiltration of different treatments were larger, but the difference was not significant. With the change of time, the upper soil water tended to be saturated, and matrix potential decreased. Capillary force and gravity became the main forces, and cumulative infiltration and wetting front process gradually became stable[39], which was consistent with the research results of most scholars[32,33]. However, the wetting front process, infiltration rate and cumulative infiltration of homogenous aeolian sandy soil were significantly higher than those of homogenous sierozem. The difference of water infiltration characteristics between sierozem and aeolian sandy soil was related to their physical and chemical properties. The sand content of aeolian sandy soil is high, and average porosity is large. The clay content of sierozem is high, and it is dominated by small pores. Soil has a large specific surface area, strong adsorption capacity for water, and good water retention[34].

Xiao Qian *et al.*[28] also pointed out that soil texture and

structure had a great influence on water infiltration parameters when studying characteristics of soil water infiltration in loess areas. Different soil types also affect its infiltration characteristics[36-38]. The stable infiltration time and rate of light sierozem[39], sandy loam, sandy soil[40], silty sandy loam[41] and silty clay loam[42] are different. Ji Hengying *et al.*[43] found that the water infiltration of homogeneous soil and layered soil in loam and sandy soil in the Loess Plateau region was significantly different after 20 – 30 min of infiltration, decreasing firstly and then increasing. The main reason was that the uneven texture of layered soil causes the abrupt change of soil water potential at the interface. When soil water permeates to the soil interface, a stagnant state appears, and the infiltration curve becomes linear; the infiltration rate tends to stabilize after the wetting front passes through the interface[44]. During the infiltration of layered soil in loess areas, the wetting front will also be disturbed due to the change of soil pores[45].

In this study, it is found that in the soil layer structure of "upper coarse sand and lower fine particles", the infiltration capacity of soil water was the highest when the thickness of coarse sand was 20 cm. In the soil layer structure of "upper fine particles and lower coarse sand", the soil permeability reduction effect was the best as the thickness of fine particles was up to 10 cm. Differences in soil type and structure are the key reasons for differences in soil water infiltration[9,46]. When the upper layer is covered with fine particles, the pores available for water flow and interconnectivity will decrease, and the curvature of water flow will increase, resulting in soil permeability reduction and increase of water retention[22,47-48]. The result of this study was consistent with the result of Li Yi *et al.*[11] (the effect of infiltration reduction was the best when the soil layer was 10 – 15 cm away from the soil surface).

General empirical model, Philip model and Kostiakov model were selected to simulate the water infiltration process of layered soil with different textures. The results show that the general empirical model had a very good fitting effect on the homogeneous sierozem and aeolian sandy soil, and the correlation coefficient reached 0.99. The Kostiakov model had a better fitting effect on the layered structure of sierozem covered with aeolian sandy soil, with the coefficient of 0.99. For the layered structure of aeolian sandy soil covered with sierozem, the fitting coefficient was slightly lower, ranging from 0.94 to 0.99, but it was still higher than that of Philip model[21]. This was consistent with the research results of many scholars[41,49].

4 Conclusions

(1) When sierozem was covered with aeolian sandy soil 5 and 10 cm thick, there was no significant difference in the wetting front process, infiltration rate and cumulative infiltration in the whole infiltration stage. As sierozem was covered with aeolian sandy soil 20 cm thick, there was a significant difference. When aeolian sandy soil was covered with sierozem 5 and 10 cm thick, there was no significant difference in the wetting front process, infiltration rate and cumulative infiltration in the initial stage of infiltration. In the stable stage of infiltration, there was a significant difference in the wetting front process, infiltration rate and cumulative infiltration as aeolian sandy soil was covered with sierozem 5, 10 and 20 cm thick. The wetting front process, (initial, stable, and average) infiltration rate and cumulative infiltration of homogenous aeolian sandy soil were significantly higher than those of homogenous sierozem.

(2) According to R^2 value and model parameters, the three infiltration models were comprehensively compared, of which the general empirical model had the best fitting effect on homogeneous soil. The order of their simulation effect on different types of layered soil was general empirical model > Kostiakov model > Philip model.

(3) The infiltration increase was the largest when sierozem was covered with aeolian sandy soil 20 cm thick[21]. That is, after a long period of desertification of sierozem, when the thickness of upper aeolian sandy soil reached more than 20 cm, the soil hydrological characteristics fundamentally changed, and the surface layer would not become the water center anymore. When the thickness of sierozem on aeolian sandy soil was 10 cm, the effect of infiltration reduction was the best. In the process of ecological restoration, the accumulation of surface fine soil reaches this depth, and the hydrological characteristics of aeolian sandy soil also change, which may no longer be suitable for the growth of deep-rooted shrubs, and vegetation succession happens. Therefore, soil type and layer thickness have a significant influence on soil infiltration process.

References

[1] SUN ZC, ZHOU YR, ZHAO YN, *et al.* Responses of soil microbial mineralization to the anthropogenic introduced shrub encroachment and water gradients in the desert steppe[J]. Acta Ecologica Sinica, 2021(4): 1 – 14.

[2] WANG J, ZHANG RQ, LI HP, *et al.* Relationship between water consumption and meteorology – vegetation parameters in the desert grassland on different time scales[J]. Agricultural Research in the Arid Areas, 2020, 38(4): 152 – 158, 167.

[3] BAO H, HOU LZ, LIU JT, *et al.* Experiment on process of soil water infiltration and redistribution under simulated rainfall[J]. Transactions of the Chinese Society of Agricultural Engineering, 2011, 27(7): 70 – 75.

[4] SUO GD, XIE YS, TIAN F, *et al.* Characteristics of soil moisture in artificial impermeable layers[J]. Chinese Journal of Applied Ecology, 2014, 25(9): 2569 – 2575.

[5] WANG XP, KANG ES, LI XR, *et al.* The influence of initial soil conditions on water penetration and soil moisture distribution[J]. Advance in Earth Science, 2003, 18(4): 592 – 596.

[6] LV G, WU XY. Review on influential factors of soil infiltration characteristics[J]. Chinese Agricultural Science Bulletin, 2008, 24(7): 494 – 499.

[7] TU AG. Advances in water infiltration and solute transport in layered soil [J]. Acta Agriculturae Universitatis Jiangxiensis, 2017, 39(4): 818 – 825.

[8] SHUAI C, XIAO MM, DAVID AB, *et al.* Model of crop growth, water flow, and solute transport in layered soil[J]. Agricultural Water Management, 2019, 221(1): 160 – 174.

[9] HILL DE, PARLANGE JY. Wetting front instability in layered soil[J]. Soil Science Society of America Journal, 1972, 36(5): 697 – 702.

[10] MILLER DE, GARDNER WH. Water infiltration into stratified soil[J]. Soil Science Society of America Journal, 1962, 26(2): 115 – 119.

[11] LI Y, REN X, ROBERT H. Effects of different textures and interlayer locations on infiltration rule of layered soil[J]. Journal of Drainage and Irrigation Machinery Engineering, 2012, 30(4): 485 -490.
[12] ROMANO N, SANTINI A. Water retention and storage: Field. Methods Soil Analysis. Part 4, Physical, Methods, 2002: 721 -738.
[13] HILLEL D, BAKER RS. A descriptive theory of fingering during infiltration into layered soils[J]. Soil Science, 1988, 146(1): 207 -217.
[14] ZHAO PL. Effects of parent material bistratification on soil water retention[M]. Journal of Northwest Institute of Soil and Water Conservation, Chinese Academy of Sciences (Special Collection on Soil Water Distribution and Soil Fertility), 1985, 2: 38 -46.
[15] REN LD, HUANG MB, FAN J. Study on water retention capacity for drained soils with different textural layering[J]. Transactions of the Chinese Society of Agricultural Engineering. 2013, 29(19): 105 -111.
[16] CHEN LX, LI FX, DI XM, *et al.* Aeolian sandy soil in China[M]. Beijing: Beijing Science Press, 1998.
[17] WANG YL, LIU LC, GAO YH, *et al.* Dynamic and spatial distribution of soil moisture in an artificially re-vegetated desert area[J]. Journal of Desert Research, 2015, 35(4): 942 -950.
[18] HUANG MB, LEE BS, ELSHORBAGY A, *et al.* Infiltration and drainage processes in multi-layered coarse soils[J]. Canadian Journal of Soil Science, 2011, 91(2): 169 -183.
[19] HUANG MB, ELSHORBAGY S, JULIE CS, *et al.* Water availability and forest growth in coarse textured soils[J]. Canadian Journal of Soil Science, 2011, 91(2): 199 -210.
[20] HUANG MB, JULIE DZ, LEE B, *et al.* The impact of soil moisture availability on forest growth indices for variably layered coarse-textured soils[J]. Ecohydrology, 2013, 6(2): 214 -227.
[21] CHEN XY. Water characteristics and factors of two typical soils in desert steppe[D]. Yinchuan: Ningxia University, 2020.
[22] XIE Q, WANG LM, QI RP, *et al.* Effects of biochar on water infi ltration and water holding capacity of loessial soil[J]. Journal of Earth Environment, 2016, 7(1): 65 -76.
[23] YE WH. Study on the relationship between soil configuration and crop growth in farmland in North China Plain[J]. Acta Geographica Sinica, 1985, 40(1): 37 -49.
[24] BAO WB, BAI YR, ZHAO YP, *et al.* Effect of biochar on soil water infiltration and water holding capacity in the arid regions of middle Ningxia [J]. Chinese Journal of Soil Science, 2018, 49(6): 1326 -1332.
[25] SONG RQ, CHU GX, YE J, *et al.* Effects of surface soil mixed with sand on water infiltration and evaporation in laboratory[J]. Transactions of the Chinese Society of Agricultural Engineering, 2010, 26(S1): 109 -114.
[26] LI Z, WU PT, FENG H, *et al.* Simulated experiment on effect of soil bulk density on soil infiltration capacity[J]. Transactions of the Chinese Society of Agricultural Engineering, 2009, 25(6): 40 -45.
[27] GAO HY, HE XS, GENG ZC, *et al.* Effects of biochar and biochar-based nitrogen fertilizer on soil water-holding capacity[J]. Chinese Agricultural Science Bulletin, 2011, 27(24): 207 -213.
[28] XIAO Q, ZHANG HP, SHEN YF, *et al.* Effects of biochar on water infiltration, evaporation and nitrate leaching in semi-arid loess area[J]. Transactions of the Chinese Society of Agricultural Engineering, 2015, 31(16): 128 -134.
[29] SHOGA GD, MEHDI H, MOHAMMAD HM, *et al.* Site-dependence performance of infiltration models[J]. Water Resources Management, 2009, 23(13): 2777 -2790.
[30] QI RP, ZHANG L, YAN YH, *et al.* Effects of biochar addition into soils in semiarid land on water infiltration under the condition of the same bulk density[J]. Chinese Journal of Applied Ecology, 2014, 25 (8): 2281 -2288.
[31] YU XX, ZHAO YT, ZHANG ZQ, *et al.* Characteristics of soil water infiltration in sub-alpine dark coniferous ecosystem of upper reaches of Yangtze River[J]. Chinese Journal of Applied Ecology, 2003, 14(1): 15 -19.
[32] YU L, ZENG C, ZE H, *et al.* Influence of soil moisture and plant roots on the soil infiltration capacity at different stages in arid grasslands of China[J]. Catena, 2019, 182(1): 1 -7.
[33] WEI YX, WANG H, LIU H, *et al.* Effect of biochar on soil moisture and its infiltration performance in black soil area[J]. Transactions of the Chinese Society for Agricultural Machinery, 2019, 50(9): 1 -14.
[34] SU YZ, YANG R, YANG X, *et al.* Effects of water-saving irrigation on cotton yield and irrigation water productivity relative to soil conditions [J]. Acta Pedologica Sinica, 2014, 51(6): 1192 -1201.
[35] NIE XY, ZHANG XC, WEI XR. Improvement of water absorbing and holding capacities of sandy soil by appropriate amount of soft rock[J]. Transactions of the Chinese Society of Agricultural Engineering, 2014, 30(14): 115 -123.
[36] LIAO CL, FU LY, SHENG H, *et al.* Natural restoration improves soil's water-storage function in abandoned dryland of purple hilly region[J]. Transactions of the Chinese Society of Agricultural Engineering, 2014, 30(21): 111 -119.
[37] QIN WJ, FAN GS. Study on influencing factors of water characteristic curve of alluvial-diluvial plain soil at low suction stage[J]. Water Saving Irrigation, 2019(10): 38 -42.
[38] SUN XQ, FANG K, FEI YH, *et al.* Structure and hydraulic characteristics of saline soil improved by applying biochar based on Micro-CT scanning[J]. Transactions of the Chinese Society for Agricultural Machinery, 2019, 50(2): 242 -249.
[39] BAI YR, ZHANG X, WANG YQ, *et al.* Study on influence of different agricultural residue film amounts on soil infiltration process of light sierozem[J]. Journal of Agricultural Resources and Environment, 2019, 36(2): 227 -235.
[40] WANG ZC, LI XY, SHI HB, *et al.* Effects of residual plastic film on infiltration and evaporation for sandy loam and sandy soil[J]. Transactions of the Chinese Society for Agricultural Machinery, 2017, 48(1): 198 -205.
[41] TIAN D. Experimental study on effects of biochar on soil structure and hydraulic characteristics of different textures[D]. Hohhot: Inner Mongolia Agricultural University, 2013.
[42] ZOU XY, NIU WQ, XU J, *et al.* Effects of residual plastic film on water infiltration and applicability analysis of infiltration models[J]. Journal of Irrigation and Drainage, 2016, 35(9): 1 -7, 12.
[43] JI HY, SHAO MA, JIA XX. Effects of water quality on infiltration of layered soils[J]. Transactions of the Chinese Society for Agricultural Machinery, 2016, 47(7): 183 -188.
[44] WANG WY, WANG QJ, SHEN B, *et al.* Infiltration characteristics of soil with doublelayer structure in Qinwangchuan area of Gansu Province [J]. Journal of Soil Erosion and Soil and Water Conservation, 1998, 4(2): 36 -40.
[45] ZHANG JF, WANG WY. Experimental study on the condition of finger flow in sand layer in loess[J]. Transactions of the Chinese Society of Agricultural Engineering, 2008, 24(3): 82 -86.
[46] COEN JR, LOUIS WD, HENDRICKX MH, *et al.* Preferential flow mechanism in a water repellent sandy soil[J]. Water Resources Research, 1993, 29(7): 2183 -2193.
[47] DOERR SH, SHAKESBY RA, WALSH RP. Soil water repellency: Its causes, characteristics and hydro-geomorphological significance [J]. Earth Science Reviews, 2000, 51(1): 33 -65.
[48] LI MY, LIU TX, LUO YY, *et al.* Study on soil infiltration process and transfer function in semi-arid steppe basin[J]. Journal of Hydraulic Engineering, 2019, 50(8): 936 -946.
[49] YAO BL, LI GY, LI FY. Soil infiltration characteristics in fallow period of drip irrigation cotton fields in south Xinjiang[J]. Scientia Agricultura Sinica, 2014, 47(22): 4453 -4462.